Molecular Neurobiology (2019) 56:7508–7521
https://doi.org/10.1007/s12035-019-1618-y

MicroRNA miR-7 and miR-17-92 in the Arcuate Nucleus of Mouse Hypothalamus Regulate Sex-Specific Diet-Induced Obesity

Yanxia Gao[1] · Jiaheng Li[2] · Zhen Zhang[1] · Ruihan Zhang[3] · Andrew Pollock[4] · Tao Sun[2,4]

Received: 29 November 2018 / Accepted: 23 April 2019 / Published online: 2 May 2019

Abstract

Proper appetite, energy expenditure, and glucose and fat metabolisms are regulated by neurons in the arcuate nucleus (ARC) of mammalian hypothalamus. Studies have shown sex-specific difference in diet-induced obesity, but the underlying mechanisms remain unclear. Here, we show that microRNA (miRNA) miR-7 and miR-17-92 are expressed in proopiomelanocortin (POMC)-expressing neurons in the mouse ARC. Specific knockdown of miR-7 and knockout of miR-17-92 in POMC-expressing neurons aggravate diet-induced obesity only in females and males, respectively. Sex-differentially expressed genes are identified in the male and female ARC of wild-type adult mice using RNA sequencing. Interestingly, some target genes for miR-7 and miR-17-92 not only display sex-differential expression in the male and female ARC but also respond to high-fat diet treatment in miR-7 knockdown and miR-17-92 knockout mice. Our results demonstrate an important role of miRNAs in regulating sex-specific diet-induced obesity, likely through modulating expression of target genes that show sex-differential expression in the ARC of the hypothalamus.

Keywords miR-7 · miR-17-92 · Obesity · POMC neurons · Sex-differential gene

Introduction

The hypothalamus is a conserved brain structure that regulates several basic life processes such as feeding, energy expenditure, sleep, and wakefulness [1–3]. The arcuate nucleus (ARC) arises from cells located in the hypothalamic ventricular zone (HVZ) through progressive proliferation, lateral migration, and differentiation [4–6]. The ARC consists of two major types of neurons: orexigenic neurons that produce neuropeptide Y (NPY) and agouti-related protein (AgRP) [7, 8] and anorexigenic neurons that produce proopiomelanocortin (POMC) and cocaine- and amphetamine-related transcript (CART) [9, 10]. POMC neurons are identified as early as embryonic day 10.5 (E10.5) in the mouse brain and their functional circuits become mature by 2 weeks old after birth [4, 11]. Studies have shown that activation of POMC neurons decreases food intake [1], affects glucose metabolism [12–14], and promotes fat burning in adulthood [15].

Interestingly, studies have shown sexual dimorphism in energy homeostasis regulated by POMC neurons in the ARC. For example, restricting POMC expression in the 5-hydroxytryptamine (serotonin) receptor 2C-positive cells in male and female mice, only male mice show hyperinsulinemia and higher capacity of fat burning [16]. Knockout of *Pten* in POMC neurons increases body weight of male mice under normal diet, while it increases body weight of female mice under high-fat diet [17]. Similarly, knockout of a transcriptionally active variant of p63 *TAp63* in POMC neurons aggravates obesity in female but not in male mice under high-fat diet [18]. Moreover, female mice have been shown to have more POMC neurons than males [18, 19], and female POMC neurons display higher firing rate than male POMC neurons [18]. The underlying mechanisms of sex-specific preference of hypothalamic functions are still unclear.

Electronic supplementary material The online version of this article (https://doi.org/10.1007/s12035-019-1618-y) contains supplementary material, which is available to authorized users.

✉ Tao Sun
taosun@hqu.edu.cn

[1] School of Life Sciences and Biotechnology, Shanghai Jiao Tong University, Shanghai 200240, China

[2] Center for Precision Medicine, School of Medicine and School of Biomedical Sciences, Huaqiao University, Xiamen 361021, Fujian, China

[3] Zhiyuan College, Shanghai Jiao Tong University, Shanghai 200240, China

[4] Department of Cell and Developmental Biology, Cornell University Weill Medical College, 1300 York Avenue, New York, NY 10065, USA

MicroRNAs (miRNA) are about 22 nucleotides small RNAs that normally affect mRNA stability or block mRNA translation by complementary sequence binding to the 3′ untranslated region (3′UTR) of their targets [20–22]. Studies have shown important roles of miRNAs in neural development and function [23–25]. Some miRNAs, for example, miR-7, let-7, and miR-124, have been found to display enriched expression in the hypothalamus [26]. Expression levels of miR-200a and miR-383a are increased in the hypothalamus of obesity models [27, 28]. Moreover, expression of miR-103 in the hypothalamus can protect mice from obtaining obesity [29], while deletion of *Dicer*, an miRNA processing enzyme, in POMC neurons results in obesity [29, 30]. These studies imply that miRNAs in the hypothalamus are involved in regulating functions of POMC neurons. However, it is unclear which specific miRNAs play a role in controlling development and function of POMC neurons.

Here we show that miR-7 and miR-17-92 are expressed in POMC-expressing neurons in the mouse brain. Knockdown of miR-7 in POMC-expressing neurons aggravates diet-induced obesity in females but not in males, and knockout of miR-17-92 in POMC-expressing neurons causes diet-induced obesity in males. Altered expression of target genes for miR-7 and miR-17-92 in the female and male ARC contributes to sex-specific obesity. Our results demonstrate a role of specific miRNAs such as miR-7 and miR-17-92 in regulating hypothalamic function, in particular in a sex-specific manner.

Materials and Methods

Experimental Animals

All experimental mice were housed in the animal facility of Shanghai Jiao Tong University. All animal experiments were approved by the Animal Ethics Committee of Shanghai Jiao Tong University.

To conditionally knock out miR-17-92 in POMC neurons, *miR-17-92*$^{flox/flox}$ mice were bred with *Pomc-Cre* mice to generate *Pomc-Cre*;*miR-17-92*$^{flox/flox}$, called *miR-17-92* KO mice [31, 32]. To conditionally knock down miR-7 in the POMC neurons, *miR-7* sponge transgenic mice were bred with *Pomc-Cre* mice to generate *Pomc-Cre*;*miR-7-sponge* lines, called *miR-7-sp* mice [33].

To visualize POMC neurons, *tdTomato* reporter transgenic mice were bred with *Pomc-Cre* mice to generate *Pomc-Cre;tdTomato* mice, in which the *tdTomato* reporter gene is activated in POMC neurons. Moreover, *Pomc-Cre;miR-7-sponge;tdTomato* (called *miR-7-sp*^{tdTomato}) mice and *Pomc-Cre;tdTomato* (named *Ctrl*^{tdTomato}) control mice were generated by crossing homozygous *tdTomato* transgenic mice with *Pomc-Cre*;*miR-7-sponge* mice. Moreover, *Pomc-Cre;miR-17-92*$^{flox/flox}$;*tdTomato* (called *miR-17-92* KO^{tdTomato}) mice and *Pomc-Cre;miR-17-92*$^{flox/+}$;*tdTomato* (named *Ctrl*^{tdTomato}) mice were generated by breeding *miR-17-92*$^{flox/flox}$ mice with *Pomc-Cre;miR-17-92*$^{flox/+}$;*tdTomato* mice.

Glucose Metabolism

The intraperitoneal glucose tolerance test (IPGTT) measures clearance of injected glucose. It has been used to measure glucose metabolism that is related to human diseases such as diabetes or metabolic syndrome [12, 34]. Briefly, mice were fasted for consecutive 16 h. Subsequently, the blood glucose level was measured as baseline. D-glucose was injected intraperitoneally with the dose of 2 g/kg body weight in mice at 16 weeks old and with the dose of 1 g/kg body weight in mice at 35 weeks old. The blood glucose level was then measured 15, 30, 45, 60, 90, and 120 min after D-glucose injection with an ACCU-CHEK active glucometer (Roche).

Tissue Preparation

For antibody staining, mouse brains at E15.5 and postnatal day 0 (P0) stages were collected directly. Adult brains were collected after perfusion of phosphate-buffered saline (PBS) and 4% paraformaldehyde in 0.1 M PBS (PFA). All brains were postfixed with 4% PFA overnight and dehydrated in 30% (*w*/*v*) sucrose for a few hours (E15.5 brains) or a few days (P0, P14 or adult brains) till brains sunk to the bottom of tubes. Dehydrated tissues embedded in O.C.T (Sakura) were sectioned (10–15 μm) by a cryostat. Coronal sections of ARC nucleus were selected under a fluorescence stereomicroscope (Leica).

For RNA extraction, brains were immediately removed after anesthetization by 3.5% chloral hydrate. Brain tissues that are anterior to the optic chiasma (OC) and posterior to mammillary body (MB) were trimmed out coronally. Coronal brain sections were collected when the mammillothalamic tract (MT) and fornix (Fx) are emerged, and were stopped until the third ventricle (3V) disappeared, using a 0.5-mm mouse stainless steel brain matrices (RWD, Shenzhen). Fresh ARC tissues were separated under a microscope with syringe needles, according to the atlas in "The Mouse Brain in Stereotaxic Coordinates." The whole collecting process was performed in cold 0.1 M PBS buffer to suppress ribonuclease activity.

Immunofluorescent Staining

Brain sections were dried at room temperature and then boiled in boiling buffer (800 ml Milli-Q water, 4 ml 1 M Tris pH 8, 1.6 ml 0.5 M for antigen recovery. Then, sections were blocked in 150 μl blocking buffer (0.1 M PBS; 10% normal goat serum (NGS) and 0.1% Tween 20) and incubated in the

first antibody (rabbit anti-RFP, 1:300) overnight. Signals were visualized using the secondary antibody (Alexa-Fluor-647, 1:300) after incubation for 1.5 h. After nucleic DNA staining by 4′,6-diamidino-2-phenylindole (DAPI), slices were mounted with fluorescent anti-fade mounting medium (Dako). Images were captured using the TCS SP8 confocal microscope (Leica).

Quantitative Real-Time Reverse Transcription PCR

Tissues were homogenized by the TRIzol reagent (Invitrogen), and total RNA was separated by chloroform and precipitated by isopropanol. After washing with 75% ethanol, the RNA pallet was dissolved in RNase-free water; 500 ng total RNA was reversely transcribed into cDNA by reverse transcriptase (TaKaRa). Quantitative PCR was performed in a qPCR machine (Bio-Rad) using SYBR green mix (TaKaRa). The primers used are shown in Table S1. The relative mRNA level was calculated by the method $2^{-\Delta\Delta T}$.

Western Blotting Assay

Fresh ARC tissues were dissected and immediately homogenized in the lysis buffer with an electric homogenizer, and total protein was extracted after centrifugation; 40 μg of total protein for each sample was loaded in a well of the SDS-PAGE gel (10% gel concentration for separation) along with the molecular weight marker. Proteins were transferred to active PVDF membrane (0.45 μm). The membrane was blocked in 5% *w*/*v* milk/TBST buffer (20 mM Tris base, 150 mM NaCl, 0.1% Tween 20, pH 7.6) for 1 h at room temperature and separately incubated in primary antibodies for Foxo1 (1:500), Bmpr1A (1:1000), and β-actin (1:500) overnight at 4 °C. After washing, the membrane was incubated in the secondary antibody (1:10,000) for 1 h at room temperature. Signals were detected using the Odyssey CLx infrared imaging system.

Statistical Analysis

For comparison of two groups, independent Student's *t* tests were performed after equality of variances was assessed by Levene's test. ANOVA analysis was used for multiple comparisons in which least significant difference (LSD) test or Dunnett's *t* test was conducted when variances were equal; otherwise, Tamhane's T2 tests were performed. All tests were two-tailed and P values < 0.05 were considered statistically significant. Values were presented as mean ± standard error mean (SEM).

Results

miR-7 Is Expressed in the Arcuate Nucleus in Developing Mouse Brains

Our previous study has shown that miRNA miR-7 is expressed in the developing mouse brain [33]. To test whether miR-7 might play a role in the ARC biological function, we first examined miR-7 expression in the ARC in developing mouse brains. Mature miR-7 consists of three family members with identical seed sequence: miR-7a1, miR-7a2, and miR-7b [33]. To distinguish expression levels of three miR-7 members in the adult mouse ARC, we conducted real-time quantitative reverse transcription PCR (qRT-PCR). miR-7a1 displayed the highest expression level among all three members, suggesting that miR-7a1 might play a major biological role in the miR-7 family (Fig. 1a).

To further verify miR-7 expression and distribution in the ARC, we performed in situ hybridization using locked nucleic acid (LNA) probes of mature miR-7. miR-7 expression was detected in E15.5 brains, including the ARC (Fig. 1b). In postnatal day 0 (P0) brains, miR-7 expression was slightly increased in the ARC compared to that in E15.5 brains (Fig. 1c). miR-7 expression was maintained in the P14 ARC (Fig. 1d). Moreover, in serial coronal sections collected from the anterior to posterior brain regions of adult mice (4 months old), miR-7 displayed high expression in the medial ARC, compared to the anterior and posterior ARC (Fig. S1).

Considering POMC neurons mainly reside in the ARC, we next examined whether miR-7 is expressed in POMC neurons. To visualize POMC neurons, *tdTomato* reporter transgenic mice were bred with *Pomc-Cre* mice to generate the *Pomc-Cre;tdTomato* line, in which most of POMC neurons will be visible under a fluorescent microscope due to specific *Pomc-Cre* activity [35] (Fig. 1e). In adult brain sections of *Pomc-Cre;tdTomato* mice, in situ hybridization was conducted using the miR-7-5p LNA probe, followed by immunohistochemistry using an anti-RFP antibody, to label miR-7 distribution and POMC-expressing neurons, respectively (Fig. 1f and Fig. S1). Images of RFP signals and miR-7 expression in the ARC were collected under the fluorescent and bright fields, respectively, and overlaid. A large number of cells (83.8% co-marked cells among RFP-positive cells, based on three individual brain sections) in the ARC were co-marked with miR-7 probes and RFP (Fig. 1g). These results suggest that miR-7 is mostly expressed in POMC-expressing neurons in the adult mouse ARC.

Knockdown of miR-7 Results in Obesity in Female Mice Under High-Fat Diet

Studies have shown that POMC neurons can be activated by nutrient-related signals such as leptin, insulin, and

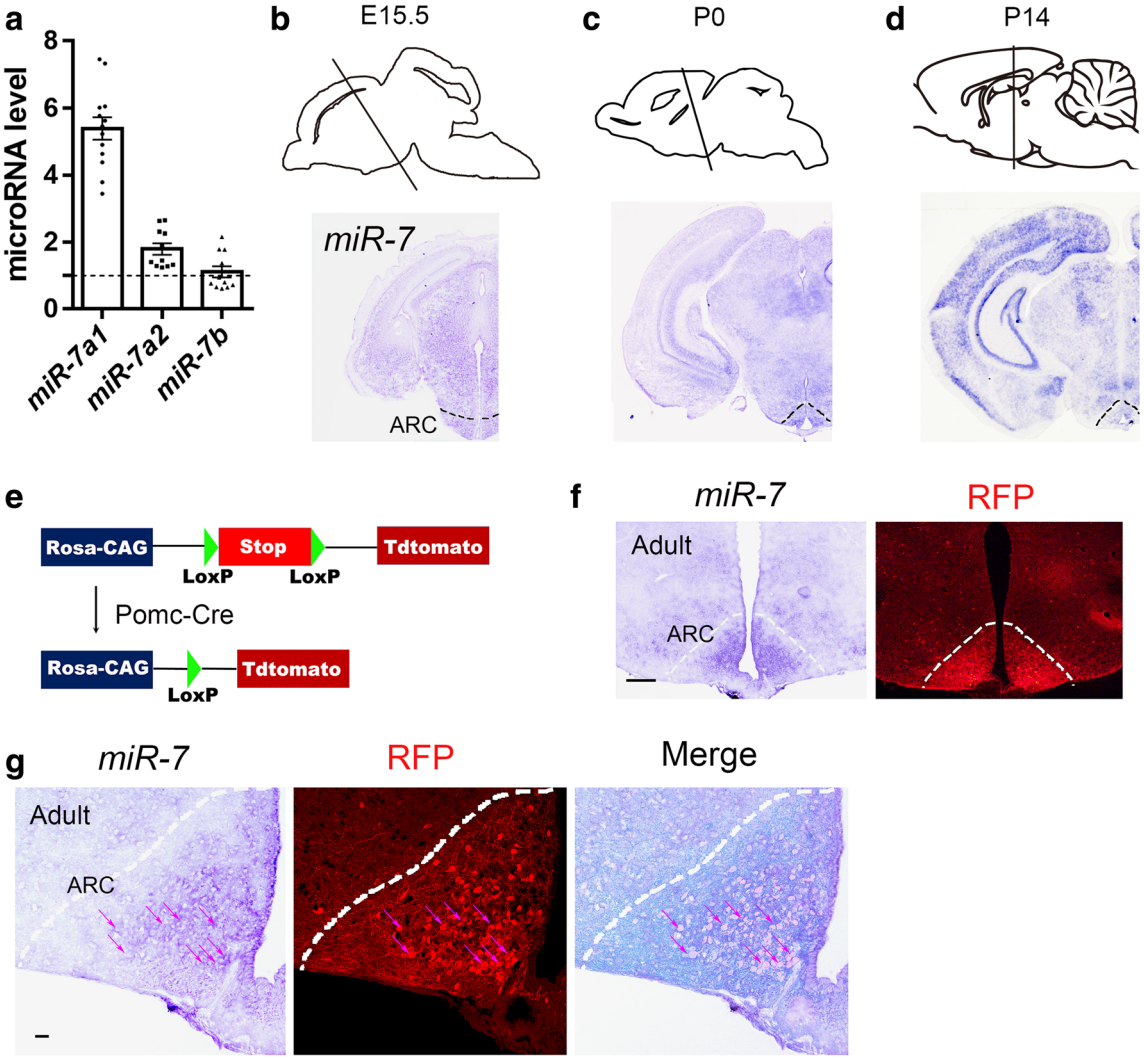

Fig. 1 *miR-7* expression in POMC neurons in the arcuate nucleus (ARC) of the mouse brain. **a** Relative expression levels of three members of the miR-7 family in the adult ARC detected by quantitative real-time reverse transcription PCR (qRT-PCR). miR-7a1 displayed the highest expression level. $n = 11–13$ brains in each group, values shown are means ± SEM. **b**–**d** miR-7 expression patterns in the ARC in E15.5, P0, and P14 brains detected by in situ hybridization. Dashed lines illustrate the ARC. **e** Diagram of generation of *Pomc-Cre*;*tdTomato* mice to visualize POMC neurons. **f** Images of miR-7 in situ hybridization (left) and RFP immunohistochemistry (right). Dashed lines illustrate the ARC. Scale bar 200 μm. **g** miR-7 was expressed in most POMC neurons in the ARC. Images of miR-7 in situ hybridization (left), RFP immunohistochemistry (middle), and merge of both (right). Dashed lines illustrate the ARC, and arrows mark neurons with co-expression of miR-7 and RFP. Scale bar 75 μm

glucose, and in turn, to repress food intake, regulate glucose metabolisms, and promote energy expenditure [4]. To examine whether knocking down miR-7 expression in POMC-expressing neurons affects energy expenditure, we applied the miRNA sponge technology, which miR-7 activity is functionally blocked by its sponges that have complementary sequence to the mature miR-7 [33]. *miR-7-sponge* transgenic mice were bred with *Pomc-Cre* mice to generate *miR-7-sp* mice, in which miR-7 is specifically knocked down in POMC-expressing neurons [33]. Wild-type and/or *miR-7-sponge* transgenic mice without *Pomc-Cre* were treated as control mice.

We first examined the number of POMC-expressing neurons in the ARC after miR-7 knockdown. To visualize POMC-expressing neurons in *miR-7-sp* mice, homozygous *tdTomato* mice were crossed with *miR-7-sp* mice to generate *Pomc-Cre;miR-7-sponge*;*tdTomato* mice (called *miR-7-sp*^{tdTomato}) and *Pomc-Cre;tdTomato* control mice (named *Ctrl*^{tdTomato}). Immunohistochemistry using the anti-RFP antibody to label POMC neurons was conducted in sections collected from the most anterior to the most posterior ARC of P0 brains. The total numbers of RFP$^+$ neurons were counted in every five sections from the anterior to posterior ARC. The numbers of RFP$^+$ POMC neurons did not show significant

difference between *miR-7-sp*^{tdTomato} and *Ctrl*^{tdTomato} mice at P0 (Fig. S2A and B). These results indicate that knockdown of miR-7 does not affect the number of POMC-expressing neurons.

We next examined whether knockdown of miR-7 in POMC-expressing neurons affects the body weight of mice under normal chow diet (NCD), and we found no significant changes of body weights in control and *miR-7-sp* mice (Fig. S3A). Interestingly, when high-fat diet (HFD) was given, *miR-7-sp* female mice displayed significantly higher weights than control females, while male mice did not show changes in body weights, even though the amount of food intake was similar between control and *miR-7-sp* mice in either males or females (Fig. 2a–c and Fig. S3B-D).

Moreover, because fat tissues were more obvious in female *miR-7-sp* mice than those in the controls, we measured body composition in female mice by magnetic resonance imaging (MRI) analysis (Fig. 2d). The fat weight and fat proportion were significantly increased in *miR-7-sp* females, compared to control females (Fig. 2e). Consequently, the lean proportion was greatly decreased in *miR-7-sp* females, compared to control females, even though the lean weight did not change (Fig. 2f). These results indicate that *miR-7* knockdown specifically aggravates obesity in females but not in males under high-fat diet.

Furthermore, under the normal chow diet condition, *miR-7-sp* and control mice were challenged by being fasted for 48 h at 16 and 35 weeks old. While there was no difference in male

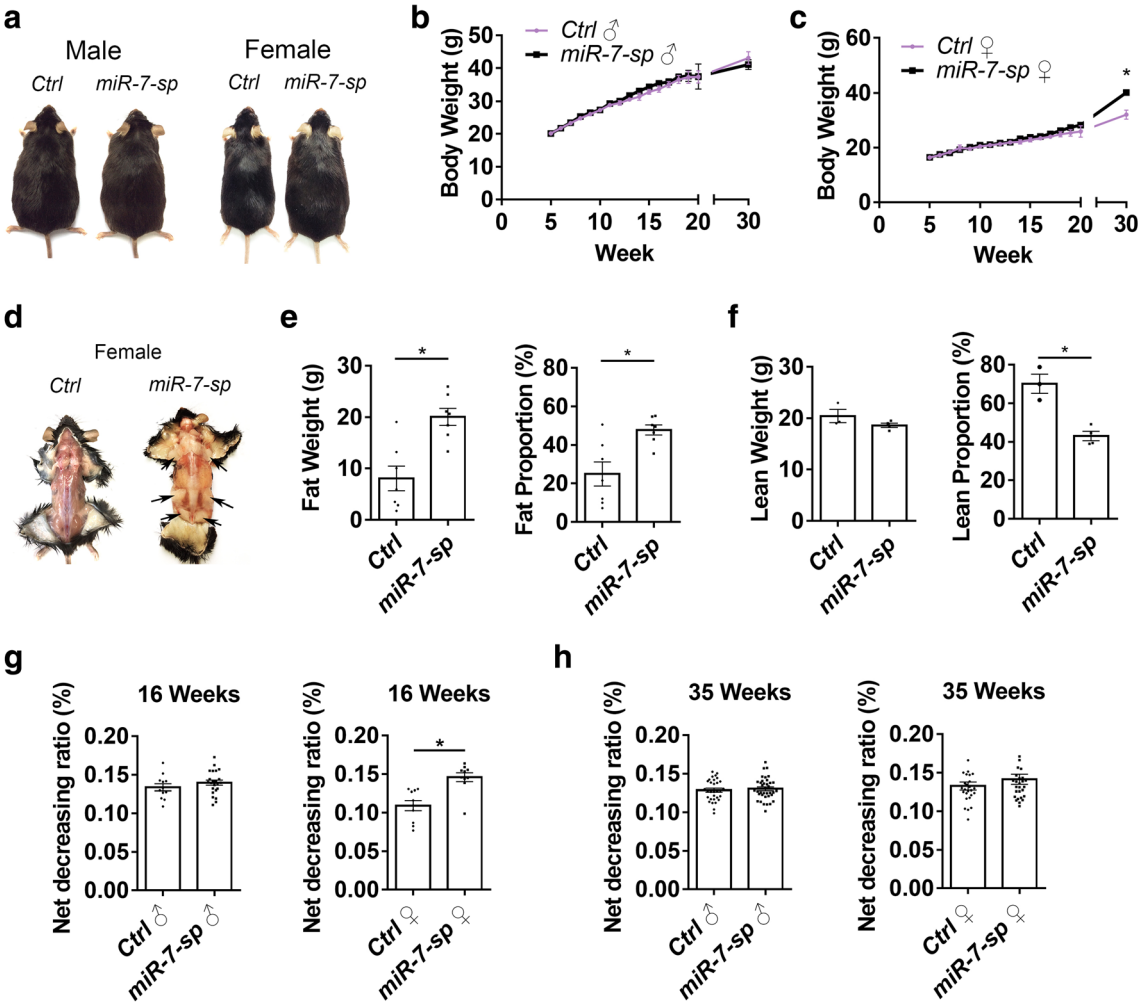

Fig. 2 Knockdown of miR-7 results in obesity in female but not in male mice under high-fat diet. **a** Images of male and female *miR-7-sp* and control (Ctrl) mice (35 weeks old) under high-fat diet (HFD). **b**, **c** Body weight of male (**b**) and female (**c**) *miR-7-sp* and control mice from 5 to 30 weeks old after treating with HFD. Compared to the same sex control mice, body weights of female *miR-7-sp* mice were increased significantly. $n = 10–28$ mice at each time point. **d** Fat tissues of female *miR-7-sp* and control mice under high-fat diet at 35 weeks old. **e**, **f** Body composition of HFD-fed female mice at 35 weeks old. Fat mass and fat proportion (fat weight/body weight) of female *miR-7-sp* mice were significantly higher than those of controls (**e**). Lean mass had no difference between female *miR-7-sp* and controls, but lean proportion of *miR-7-sp* mice was significantly lower than that of controls (**f**). $n = 3–7$ mice in each group. **g**, **h** Changes in body weights after fasting for 48 h at 16 weeks (**g**) and 35 weeks (**h**) under normal chow diet. The ratio of body weight decrease in female *miR-7-sp* mice was more than controls at 16 weeks old. $n = 9–22$ mice in each group. Values shown are means ± SEM. $^*P < 0.05$, Student's *t* test

mice, *miR-7-sp* female mice showed a higher ratio of weight decrease than control females at 16 weeks old (Fig. 2g). And the weight decrease in *miR-7-sp* female mice was recovered at 35 weeks old (Fig. 2h). These data suggest that knockdown of miR-7 transiently affects response to food fasting in female but not in male mice.

To further examine whether the sex difference might be due to miR-7 expression levels in the ARC at different developmental stages, we quantified miR-7 expression in the male and female ARCs using qRT-PCR. In the ARCs of 15-, 25-, and 35-week-old brains, miR-7a1 expression levels were slightly decreased with ages but had no significant difference in male and female ARCs at each stage (Fig. S4A). Moreover, *miR-7a1* expression patterns also did not show changes in the ARCs at different stages as detected by in situ hybridization (Fig. S4C). These results suggest that sex difference in male and female *miR-7-sp* mice upon HFD treatment is not caused by different miR-7 expression in the male and female ARCs.

Knockdown of miR-7 Affects Glucose Metabolism

The IPGTT that measures blood glucose clearance is used to assess glucose metabolism [12, 34]. To investigate whether miR-7 knockdown affects glucose metabolism, we conducted the IPGTT in *miR-7-sp* and control mice under normal chow diet. Interestingly, after 15, 30, 45, and 60 min of glucose injection, 18-week-old female *miR-7-sp* mice showed lower glucose levels than the same aged controls, while male *miR-7-sp* mice displayed compatible levels with controls (Fig. S3E). However, neither female nor male *miR-7-sp* mice showed difference at 35 weeks old (Fig. S3F). These results suggest that knockdown of miR-7 results in periodic stronger abilities to glucose clearance in female but not in male mice.

Furthermore, we conducted the IPGTT in *miR-7-sp* and control mice under high-fat diet. Opposite to the normal chow diet conditions, after 30, 60, and 90 min of glucose injection, 18-week-old male *miR-7-sp* mice showed lower glucose levels than the same aged controls, while female *miR-7-sp* mice displayed compatible levels with controls (Fig. S3G). Neither female nor male *miR-7-sp* mice showed difference at 35 weeks old (Fig. S3H). These data suggest that under high-fat diet, knockdown of miR-7 causes periodic stronger abilities to glucose clearance in male but not in female mice. These results also hint that miR-7 regulates glucose metabolism in a sex-specific manner.

MicroRNA miR-17-92 Cluster Is Expressed in POMC-Expressing Neurons

To extend our study of miRNA regulation in the ARC, we examined the expression of another miRNA, the miR-17-92 cluster, in the ARC [31, 32]. We first examined the expression levels of three miRNAs in the miR-17-92 cluster in the adult ARC using qRT-PCR [31]. miR-92a displayed the highest expression level among all three members (Fig. 3a). We then validated the expression patterns of miR-17, miR-19a, and miR-92a using in situ hybridization. All three miRNAs were expressed in the ventral hypothalamus, including the ARC, in E15.5 and P0 brains (Fig. S5A and 5B). In serial coronal sections collected from the anterior to posterior brain regions of adult mice, all three miRNAs displayed high expression in the posterior ARC, compared to the anterior and medial ARC (Fig. 3b and Fig. S5C).

We further examined miR-92a expression in POMC neurons using the *Pomc-Cre;tdTomato* line. In brain sections of *Pomc-Cre;tdTomato* mice, in situ hybridization was conducted using the miR-92a LNA probe to confirm miR-92a distribution, followed by immunohistochemistry using anti-RFP antibodies to label POMC neurons. Images of RFP signals and miR-92a expression in the ARC were collected under the fluorescent and bright fields, respectively, and overlaid. Majority of cells (88.2% co-marked cells in RFP-positive cells, based on three individual brain sections) in the ARC were co-marked with RFP and miR-92a probes (Fig. 3c). These results imply that miR-92a might be a major player in miR-17-92 and regulates the development of POMC-expressing neurons.

Distinct Body Weight Changes in Male and Female *miR-17-92* KO Mice Under High-Fat Diet

Considering that miR-17-92 is expressed in POMC-expressing neurons in the ARC, we suspected that miR-17-92 might also play a role in regulating body weights. Floxed miR-17-92 transgenic mice ($miR\text{-}17\text{-}92^{flox/flox}$) were bred with *Pomc-Cre* mice to generate conditional *miR-17-92* knockout mice, in which miR-17-92 is only deleted in POMC-expressing cells, named *miR-17-92* KO [31, 32].

We first examined the number of POMC-expressing neurons in *miR-17-92* KO mice. $Pomc\text{-}Cre;miR\text{-}17\text{-}92^{flox/flox};tdTomato$ mice (called $miR\text{-}17\text{-}92\ KO^{tdTomato}$) and $Pomc\text{-}Cre;miR\text{-}17\text{-}92^{flox/+};tdTomato$ mice (named $Ctrl^{tdTomato}$) were generated by breeding $miR\text{-}17\text{-}92^{flox/flox}$ mice with $Pomc\text{-}Cre;miR\text{-}17\text{-}92^{flox/+};tdTomato$ mice. Immunohistochemistry using anti-RFP antibodies to label POMC neurons was conducted and the total numbers of RFP^+ neurons were counted in every five sections from the anterior to posterior ARC in P0 brains. The number of RFP^+ POMC neurons did not show significant changes between *miR-17-92* KO and control mice (Fig. S2C and D). These results indicate that *miR-17-92* knockout does not affect the number of POMC neurons.

Similar to *miR-7* knockdown mice, under normal chow diet, *miR-17-92* KO mice did not show significant changes in body weights between control and *miR-17-92* KO mice in either males or females (Fig. S6A). Interestingly, high-fat diet affected body weights in both male and female *miR-17-92* KO

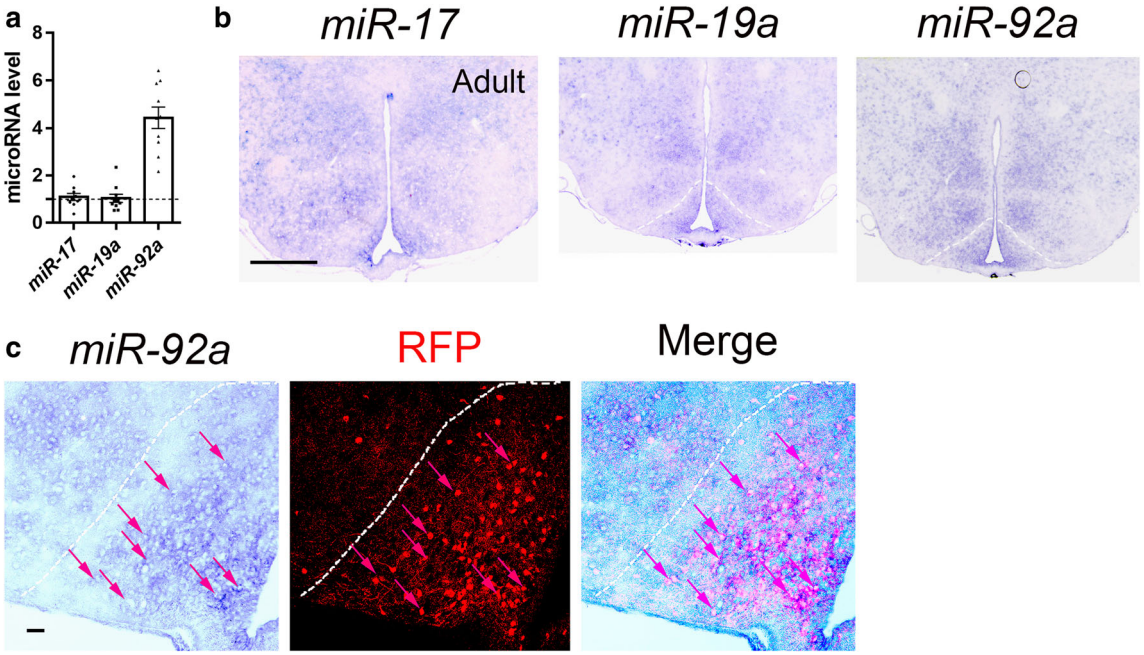

Fig. 3 *miR-17-92* expression in POMC neurons in adult mouse brains. **a** Relative expression level of three members in the miR-17-92 family in the adult ARC detected by real-time qRT-PCR. $n = 9–10$ brains in each group. **b** miR-17, 19a, and 92a expression in the adult ARC detected by in situ hybridization. Dashed lines illustrate the ARC. Scale bar 500 μm. **c** miR-92a was expressed in most POMC neurons in the ARC. Images of miR-92a in situ hybridization (left), RFP immunohistochemistry (middle), and merge of both (right). Dashed lines illustrate the ARC, and arrows mark neurons with co-expression of miR-92a and RFP. Scale bar 75 μm

mice, with male *miR-17-92* KO mice heavier than male controls, and female *miR-17-92* KO mice lighter than female controls, when the amount of food intake was similar between control and *miR-17-92* KO mice (Fig. 4a, b, and Fig. S6B). The body weight change occurred earlier in male than female *miR-17-92* KO mice (displayed weight gain at 15 weeks and weight loss at 20 weeks, respectively) (Fig. 4a, b).

Moreover, the fat weight and proportion were higher in male *miR-17-92* KO mice than those in male controls, and the lean proportion was less in male *miR-17-92* KO mice than those in male controls (Fig. 4c, d). Oppositely, the fat weight and proportion were less in female *miR-17-92* KO mice than those in female controls, and the lean proportion was higher in female *miR-17-92* KO mice than those in female controls (Fig. 4e, f). These results indicate that high-fat diet affects both males and females when miR-17-92 is deleted in POMC-expressing cells, with gain-of-fat weight in male KO and loss-of-fat weight in female KO.

Furthermore, unlike miR-7 knockdown mice, fasting for 48 h did not affect body weights in either male or female *miR-17-92* KO mice (Fig. S6C and D). Additionally, in the IPGTT, blood levels after glucose injection showed no significant changes between *miR-17-92* KO and control mice under high-fat diet, whether males or females (Fig. S6E and F). These data suggest that miR-17-92 knockout does not change the capacity of glucose clearance and glucose metabolism.

Finally, we examined whether the sex difference might be due to miR-92a expression levels in the ARC at different developmental stages, and quantified miR-92a expression in the male and female ARCs using qRT-PCR. In the ARCs of 15-, 25-, and 35-week-old brains, miR-92a expression levels did not display significant differences between male and female ARCs at each stage (Fig. S4B). *miR-92a* expression patterns also did not show changes in the ARCs at different stages (Fig. S4D). These results suggest that sex difference in male and female *miR-17-92* mice upon HFD treatment is not caused by different miR-92a expression in the male and female ARCs.

Differential Gene Expression in the Male and Female ARC

Because male and female *miR-7-sp* and *miR-17-92* KO mice showed differential response in body weight under high-fat diet (Figs. 2 and 4), we speculated that gene expression in the ARC might display sex-specific differences. To test this idea, we analyzed gene expression profiles in ARCs in wild-type adult male and female mouse brains using RNA sequencing analysis (Fig. 5a). Among differentially expressed genes in the male and female ARCs (male versus female), genes with fold changes less than 0.77 were considered as male low-expression genes (i.e., female high-expression genes), while genes with fold

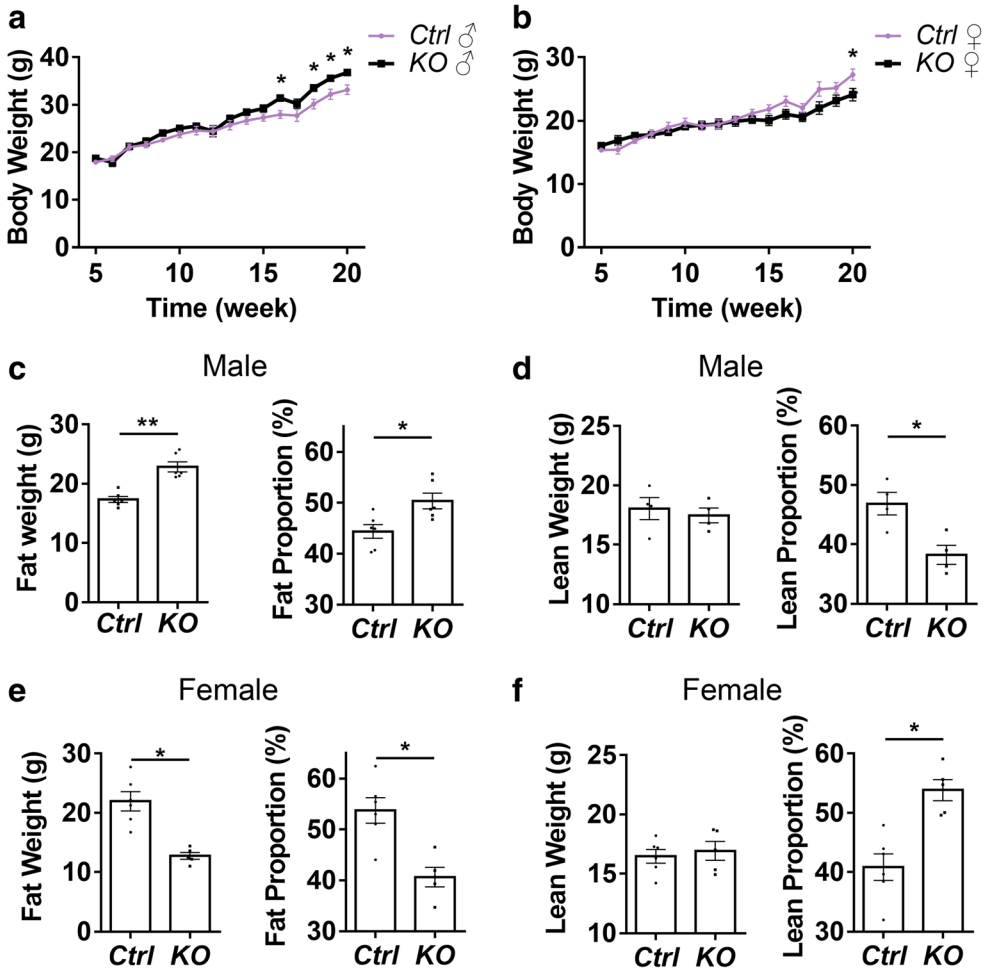

Fig. 4 Distinct body weight changes in male and female *miR-17-92* knockout (KO) mice under high-fat diet (HFD). **a**, **b** Body weight of male (**a**) and female (**b**) *miR-17-92* KO and control (Ctrl) mice from 5 to 20 weeks old after treating with HFD. Compared to the same sex control mice, body weights of male *miR-17-92* KO mice were significantly increased, while body weights of female *miR-17-92* KO mice were significantly decreased. $n = 6$–14 mice at each time point. **c**, **d** Body composition of HFD-fed male mice at 25 weeks old. Fat mass and fat proportion (fat weight/body weight) of male *miR-17-92* KO mice were significantly higher than those of controls. Lean mass had no difference between male *miR-17-92* KO and controls, but lean proportion of *miR-17-92* KO mice was significantly lower than that of controls. $n = 4$–6 mice in each group. **e**, **f** Body composition of HFD-fed female mice at 25 weeks old. Fat mass and fat proportion (fat weight/body weight) of female *miR-17-92* KO mice were significantly lower than those of controls. Lean mass had no difference between female *miR-17-92* KO and controls, but lean proportion of *miR-17-92* KO mice was significantly higher than that of controls. $n = 5$–6 mice in each group. Values shown are means ± SEM. $^*P < 0.05$; $^{**}P < 0.01$, Student's *t* test

changes more than 1.3 were considered as female low-expression genes (i.e., male high-expression genes).

In the male and female ARCs, while 10,478 genes showed no differential expression between males and females, 2957 (~22%) genes displayed sex-biased expression, with 1641 genes showing male low expression and 1316 genes showing female low expression (Fig. 5a).

Moreover, the Gene Ontology (GO) analysis (https://david.ncifcrf.gov) was performed in 2957 sex-differentially expressed genes (SDEGs). In the biological process (BP) category, 409 genes (about 13.8%) were detected to be involved in the regulation of transcription, suggesting a role of gene expression regulation of SDEGs (Fig. S7A).

Target Genes for miR-7 and miR-17-92 Show Sex-Differential Expression

Given that female *miR-7-sp* mice displayed obvious obesity, we explored whether predicted target genes for miR-7 in the ARC in *miR-7-sp* brains show sex-differential expression. Among 331 predicted targets, 20 genes showed male low expression, i.e., female high expression, while 157 genes displayed female low expression, i.e., male high expression (Fig. 5b). Because miRNAs normally silence target gene expression, these data suggest that miR-7 knockdown may cause upregulation of genes that normally have low expression in the female ARC. Moreover, the GO-BP analysis based on 157 female

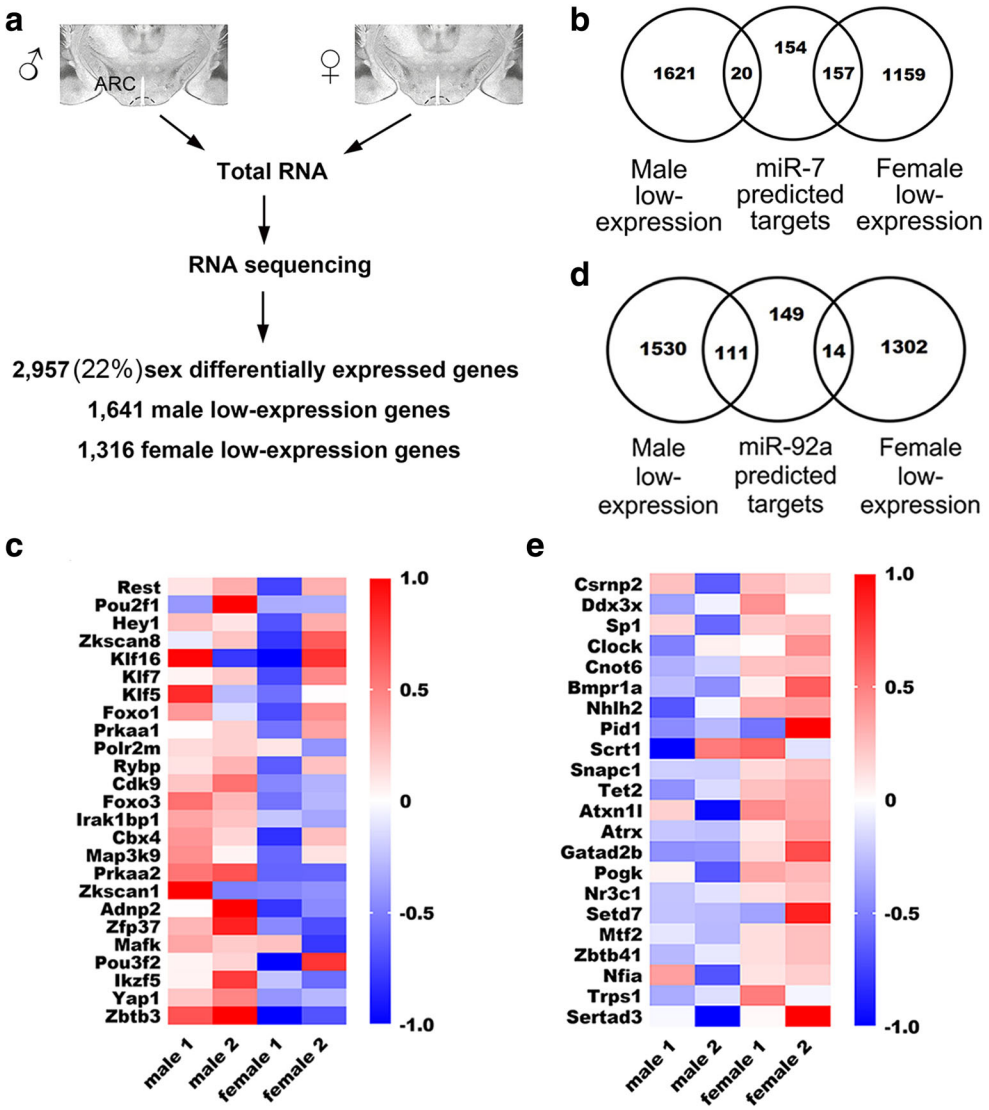

Fig. 5 Target genes for miR-7 and miR-17-92 show sex-differential expression. **a** Differential gene expression in the male and female ARC analyzed by RNA sequencing; 2957 genes displayed sex-differential expression, with 1641 genes showing male low expression and 1316 genes showing female low expression. **b** Venn diagram of sex-differentially expressed genes and predicted target genes for miR-7. **c** Heatmap of gene expression levels of the "transcription, DNA-templated" group in the GO-BP analysis of the 157 genes, which are miR-7 predicted targets and also show female low expression in the ARC. **d** Venn diagram of sex-differentially expressed genes and predicted targets for miR-92a. **e** Heatmap of gene expression levels of the "transcription, DNA-templated," "regulation of transcription, DNA-templated," and "positive regulation of transcription from RNA polymerase II promoter" groups in the GO-BP analysis of the 111 genes, which are 92a predicted targets and also show male low expression in the ARC

low-expression genes identified 25 genes that function in regulating transcription (Fig. 5c and Fig. S7B).

Similarly, because female and male *miR-17-92* KO mice showed distinct responses toward HFD (Fig. 4), we explored whether predicted target genes for miR-92a show sex-differential expression as well. Among 274 predicted targets, 111 genes showed male low expression, and 14 genes displayed male high expression (Fig. 5d). These results suggest that *miR-17-92* knockout may result in the upregulation of genes that normally have low expression in the male ARC. The GO-BP analysis of 111 male low-expression genes further identified 22 genes that are involved in transcription regulation (Fig. 5e and Fig. S7C). These results suggest that some target genes for miR-7 and miR-17-92 display sex-differential expression and function in regulating transcription of other genes.

Altered Expression of miR-7 and miR-17-92 Affects Sex-Differentially Expressed Genes in the ARC

To validate the expression levels of sex-differentially expressed genes, real-time qRT-PCR was performed. As examples, *Foxo1*, *Fbxo45*, and *Rybp* showed higher levels in the male ARC than in females in wild-type mouse brains, while

Ddx3x, *Bmpr1A*, and *Clock* displayed higher levels in females than males (Fig. 6a).

To examine whether female low-expression genes respond to HFD treatment, we quantified the *Foxo1* expression level by qRT-PCR in male and female *miR-7-sp* and control mice fed with HFD. We detected elevated *Foxo1* expression in the ARC of female *miR-7-sp* mice, compared to their same sex controls, while there were no detectable changes in the ARC of male *miR-7-sp* and their same sex controls (Fig. 6b). In addition, it has been shown that Foxo1 can repress Pomc level in POMC neurons [36], so we quantified *Pomc* expression level by qRT-PCR. While there was no difference in male *miR-7-sp* and control mice, there was a significant reduction of *Pomc* expression in the ARC of female *miR-7-sp* mice, compared to their same sex controls, upon HFD treatment (Fig. 6c). These results suggest that upregulation of genes that normally show low expression in the ARC of female brains might contribute to female-specific obesity when miR-7 is knocked down.

Moreover, because miR-17-92 plays a role in brain neurogenesis [31, 32, 37], we examined the expression levels of sex-differentially expressed genes that are associated with neurogenesis such as *Ki67* and *Bdnf* in the ARC of *miR-17-92* control and KO mice upon HFD treatment. While there was no difference in male control and *miR-17-92* KO mice, there was a significant increase of *Ki67* and *Bdnf* expression in the ARC of female *miR-17-92* KO mice, compared to their same sex controls (Fig. 6d). In addition, FoxA1 has been shown to act as a key factor for both androgen receptor (AR) and estrogen receptor-α (ER) to mediate sexual dimorphism [38–42];

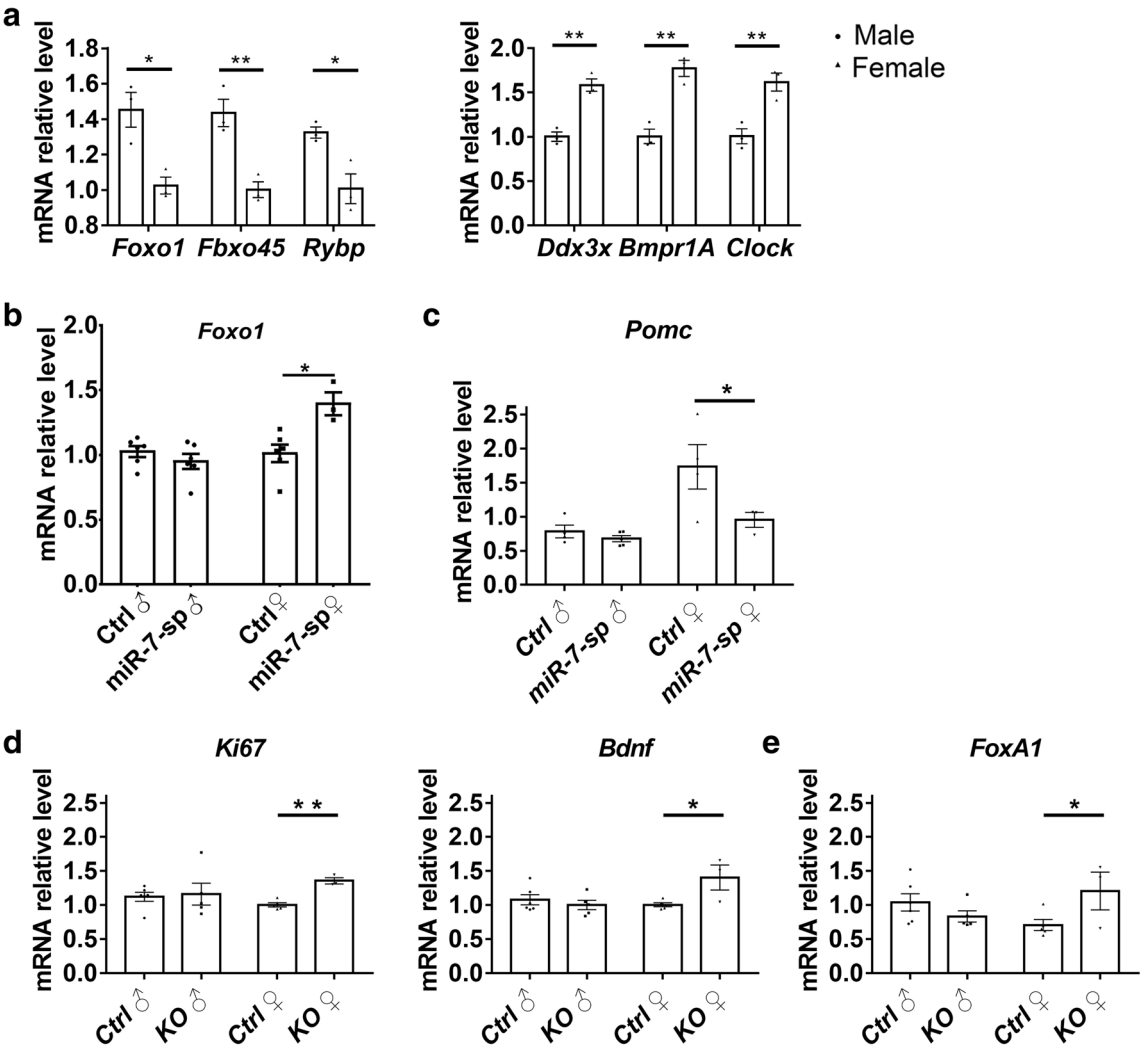

Fig. 6 Altered expression of miR-7 and miR-17-92 affects sex-differentially expressed genes in the ARC. **a** Validation of expression levels of sex-differentially expressed genes in the ARC by real time qRT-PCR, including female low-expressed genes *Foxo1*, *Fbxo45*, and *Rybp* and male low-expressed genes *Ddx3x*, *Bmpr1A*, and *Clock*. $n = 3$ brains for each group. **b**, **c** The relative expression level of *Foxo1* (**b**) and *Pomc* (**c**) in the ARC of high-fat diet-fed *miR-7-sp* and control mice detected by real-time qRT-PCR. $n = 3$–6 brains for each group. **d**, **e** The relative expression level of *ki67*, *Bdnf* (**d**), and *FoxA1* (**e**) in the ARC of high-fat diet-fed miR-17-92 KO and control mice detected by real-time qRT-PCR. $n = 3$–6 brains for each group. Values shown are means ± SEM. $^*P < 0.05$; $^{**}P < 0.01$, Student's *t* test (**a**) and ANOVA test (**b**–**e**)

we, thus, measured its expression. We found elevated *FoxA1* expression in the ARC of female *miR-17-92* KO mice, compared to their same sex controls, while there were no detectable changes in the ARC of male *miR-17-92* KO and their same sex controls (Fig. 6e). These data suggest that sex-specific responses to HFD in *miR-17-92* KO might be due to distinct altered expression of genes that normally show sex-differential expression in the ARC.

Sex-Differential Expression at the Protein Level

To further validate the expression levels of sex-differentially expressed genes, we conducted Western blotting assay. Consistent with mRNA levels quantified by real-time qRT-PCR (Fig. 6a), Foxo1 protein level was higher in the male adult ARC than in the female, while Bmpr1A protein level was lower in the male ARC than in the female in wild-type mouse brains (Fig. 7a, b).

Moreover, we validated Foxo1 expression in the female ARC in wild-type and *miR-7-sp* mice treated with high-fat diet using immunohistochemistry. Anti-NeuN antibody was used to label mature neurons. We found that the proportion of Foxo1-expressing cells versus NeuN$^+$ cells was significantly increased in the ARC in female *miR-7-sp* brains, compared to female control brains (Fig. 7c, d). The proportion of Foxo1/NeuN double-positive cells versus NeuN$^+$ cells also was increased in the ARC in female *miR-7-sp* brains (Fig. 7c, d). These results suggest that elevated expression of Foxo1 protein in the ARC of female *miR-7-sp* mice contributes to female-specific obesity.

Discussion

Energy expenditure and obesity are regulated by the hypothalamus, in particular, the ARC that consists of POMC neurons. Studies have shown that POMC neurons modulate sex-specific changes of body weights in diet-induced obesity [16, 43, 44]. Here, we show that specific miR-7 knockdown and miR-17-92 knockout mice in POMC-expressing neurons display sex-different response to high-fat diet. We further demonstrate that altered expression of genes that normally show high- or low-expression levels in the ARC of male or female mice is associated with sex-specific obesity.

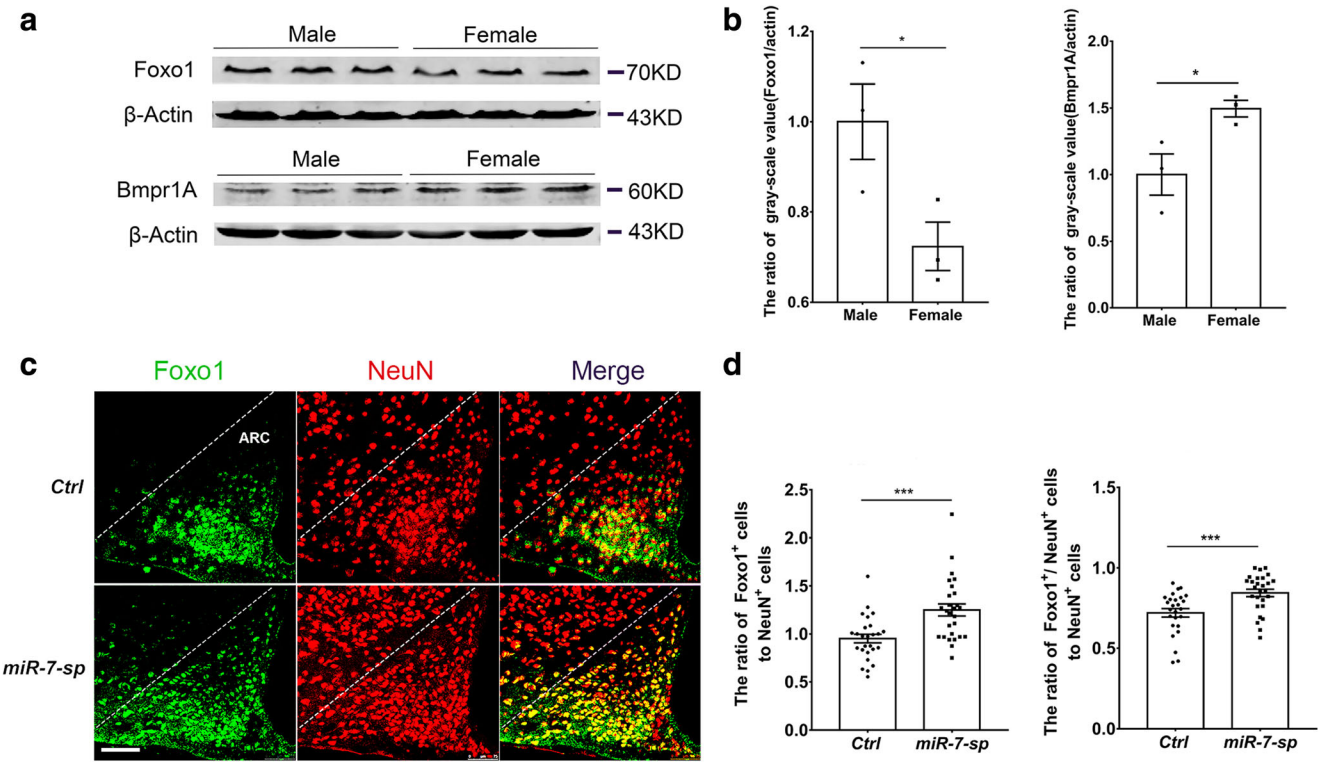

Fig. 7 Protein expression of sex-differentially expressed genes. **a** Western blotting assay of Foxo1 and Bmpr1A in the male and female ARCs in wild-type adult mouse brains. **b** Quantification of Foxo1 and Bmpr1A expression levels. More Foxo1 protein was detected in the male ARC than in the female, while less Bmpr1A protein was detected in the male ARC than in the female. $n = 3$ brains for each group. **c** Foxo1 expression (green color) detected by immunohistochemistry in the female ARC in wild-type and *miR-7-sp* mice treated with high-fat diet. Anti-NeuN antibody was used to label mature neurons (red color). Dashed lines illustrate the ARC. **d** The proportion of Foxo1-expressing cells versus NeuN$^+$ cells was significantly increased in the ARC in female *miR-7-sp* brains, compared to female control brains. The proportion of Foxo1/NeuN double-positive cells versus NeuN$^+$ cells also was increased in the ARC in female *miR-7-sp* brains. $n = 30$ sections from at least three brains in each group. Values shown are means ± SEM. $^*P < 0.05$, $^{***}P < 0.001$, Student's *t* test. Scale bar 75 μm

Accumulating evidence has shown important roles of miRNAs in regulating body weights. For example, long-time systemic inhibition of miR-21 can relieve obesity in leptin receptor-deficient (*db/db*) mice by decreasing the adipocyte size and serum triglycerides [45], and *miR-155* knockout specifically protects high-fat diet-induced obesity in female mice by increasing energy expenditure [46]. Furthermore, miR-219 conditional knockdown in the ventromedial hypothalamus (VMH), which also participates in obesity and energy expenditure, increases the risk of obesity, while miR-219 overexpression relieves diet-induced obesity [47]. Our study here shows that miR-7 and miR-17-92 not only regulate body weight, glucose consumption, and diet-induced obesity but also display a sex preference manner.

MiRNA miR-7 is crucial for neural development and function. Knocking down miR-7 using the miRNA sponge specifically in the cortex causes a smaller brain due to altered neural progenitor proliferation and differentiation [33]. Studies have shown that miR-7 binds to circular RNA *Cdr1as* to modulate brain functions [48]. Moreover, the miR-17-92 cluster plays essential roles in controlling expansion of neural stem cells and neural progenitors and, in turn, the brain size [31, 49]. miR-17-92 also regulates mood-associated behaviors by maintaining adult neural stem cell proliferation [32]. Here, we show that both miR-7 and miR-17-92 play a role in regulating ARC-related body weight control. We have found that knocking down miR-7 and knocking out miR-17-92 specifically in the ARC do not affect the number of POMC neurons, suggesting a distinct role of these miRNAs in the cortex and hypothalamus. These results also imply that altered gene expression by miR-7 and miR-17-92 in POMC neurons, instead of their number, is crucial for hypothalamus function. Furthermore, *miR-7* knockdown and *miR-17-92* knockout mice do not show body weight changes under normal chow diet, while they display obesity under high-fat diet. Our results support the perspective view of miRNA functions: while miRNAs play robust roles in developmental processes, they also excel functions in a tissue-specific manner, in particular under stress conditions [50, 51].

Interestingly, we have found that only female *miR-7* knockdown mice and male *miR-17-92* knockout mice display diet-induced obesity. Previous reports have shown sex-specific changes of body weights, which is regulated by POMC neurons [16, 43, 44]. However, how POMC neurons modulate sex-specific changes of body weight is unclear. Here, we have found that some genes display differential expression levels in the male and female ARCs in wild-type mouse brains. How sex-differential expression of these genes are established and whether their expressions are maintained by hormone or other factors are still unclear [16, 17]. Because miRNAs normally function through silencing target genes, genes upregulated in the ARCs of *miR-7* knockdown and *miR-17-92* knockout brains are likely potential targets for these miRNAs. Interestingly, we have found that some target genes for miR-7 and miR-17-92 are enriched in sex-differentially expressed genes. In particular, miR-7 target genes, which normally show low expression in female wild-type ARCs, are upregulated in female ARCs of *miR-7-sp* mice, while miR-92 target genes, which normally display low expression in male wild-type ARCs, are upregulated in male ARCs of *miR-17-92* knockout mice. The gene expression profile shift of sex-differentially expressed genes in male or female ARCs, caused by altered miR-7 and miR-17-92 expression, might contribute to sex-specific body weight changes. The future study should examine why and how female and male ARCs display gene expression changes upon miR-7 knockdown and miR-17-92 knockout, respectively.

Because of the feature of miRNAs in silencing target genes, it is likely that sex-specific body weight changes in *miR-7* knockdown and *miR-17-92* knockout mice are caused by altered expression of targets for miR-7 and miR-17-92. Studies have shown that decreased Pomc level can induce obesity [10, 52]. And the Pomc level is usually repressed by Foxo1 [36]. We have found elevated expression of Foxo1 in the female but not in male ARC in *miR-7* knockdown brains, which implies potential regulatory consequence of Foxo1 and Pomc levels and the body weight change. Furthermore, FoxA1 has been reported to mediate sexual dimorphism [38, 39]. We here have found increased *FoxA1* level in the female but not in male ARC in *miR-17-92* knockout brains. Furthermore, because one miRNA can have many targets, it is likely that sex-specific body weight changes are a result of alteration of multiple gene pathways, which are normally repressed by miR-7 and miR-17-92. Our RNA-seq data of a group of sex-differentially expressed genes also support this possibility. The future work should dissect major miRNA targets that mediate sex-specific functions of the hypothalamus.

Taken together, our studies have shown that miR-7 and miR-17-92 play crucial roles in regulating body weight and glucose consumption, which are mediated by POMC-expressing neurons in the ARC of the hypothalamus. Importantly, miR-7- and miR-17-92-mediated body weight control upon high-fat diet treatment displays a sex-specific feature, which is likely caused by altered expression of sex-differential genes in the ARC. Our study should shed new light on preventive investigation of obesity in the future.

Acknowledgments We thank the members of the Sun Laboratory for their valuable discussions and advice.

Authors' Contribution Conceived and designed the experiments: Y.G. and T.S.; experiment: Y.G., Z.Z., and A.P.; result analysis: Y.G., J.L., and R.Z.; wrote the paper: Y.G. and T.S; edited the paper: T.S.

Funding Information This work was supported by an R01-MH083680 grant from the NIH/NIMH (T. S.) and the National Natural Science Foundation of China (81471152 and 31771141).

Compliance with Ethical Standards

All animal experiments were approved by the Animal Ethics Committee of Shanghai Jiao Tong University.

Conflict of Interest The authors declare that they have no conflict of interest.

References

1. Clifford BS, Bradford BL (2015) The hypothalamus. Curr Biol 24(23)
2. Dietrich MO, Horvath TL (2013) Hypothalamic control of energy balance: insights into the role of synaptic plasticity. Trends Neurosci 36(2):65–73. https://doi.org/10.1016/j.tins.2012.12.005
3. Saper CB, Scammell TE, Lu J (2005) Hypothalamic regulation of sleep and circadian rhythms. Nature 437(7063):1257–1263. https://doi.org/10.1038/nature04284
4. Toda C, Santoro A, Kim JD, Diano S (2017) POMC neurons: from birth to death. Annu Rev Physiol 79(79):209–236. https://doi.org/10.1146/annurev-physiol-022516-034110
5. Mcclellan KM, Calver AR, Tobet SA (2008) GABA(B) receptors role in cell migration and positioning within the ventromedial nucleus of the hypothalamus. Neuroscience 151(4):1119–1131. https://doi.org/10.1016/j.neuroscience.2007.11.048
6. Shimogori T, Lee DA, Miranda-Angulo A, Yang Y, Wang H, Jiang L, Yoshida AC, Kataoka A et al (2010) A genomic atlas of mouse hypothalamic development. Nat Neurosci 13(6):767–U153. https://doi.org/10.1038/nn.2545
7. Joly A, Denis R, Castel J, Palmiter R, Magnan C, Luquet S (2010) Role of neural NPY/AgRP in the control of energy balance. Diabetes Metab 36:A10–A10. https://doi.org/10.1016/S1262-3636(10)70039-2
8. Mercer RE, Chee MJ, Colmers WF (2011) The role of NPY in hypothalamic mediated food intake. Front Neuroendocrinol 32(4):398–415. https://doi.org/10.1016/j.yfrne.2011.06.001
9. Gao Y, Sun T (2016) Molecular regulation of hypothalamic development and physiological functions. Mol Neurobiol 53(7):4275–4285. https://doi.org/10.1007/s12035-015-9367-z
10. Greenman Y, Kuperman Y, Drori Y, Asa SL, Navon I, Forkosh O, Gil S, Stern N et al (2013) Postnatal ablation of POMC neurons induces an obese phenotype characterized by decreased food intake and enhanced anxiety-like behavior. Mol Endocrinol 27(7):1091–1102. https://doi.org/10.1210/me.2012-1344
11. Coupe B, Bouret SG (2013) Development of the hypothalamic melanocortin system (POMC). Front Endocrinol 4:38. https://doi.org/10.3389/fendo.2013.00038
12. Parton LE, Ye CP, Coppari R, Enriori PJ, Choi B, Zhang CY, Xu C, Vianna CR et al (2007) Glucose sensing by POMC neurons regulates glucose homeostasis and is impaired in obesity. Nature 449(7159):228–U227. https://doi.org/10.1038/Nature06098
13. Smith MA, Katsouri L, Irvine EE, Hankir MK, Pedroni SMA, Voshol PJ, Gordon MW, Choudhury AI et al (2015) Ribosomal S6K1 in POMC and AgRP neurons regulates glucose homeostasis but not feeding behavior in mice. Cell Rep 11(3):335–343. https://doi.org/10.1016/j.celrep.2015.03.029
14. Berglund ED, Vianna CR, Donato J, Kim MH, Chuang JC, Lee CE, Lauzon DA, Lin P et al (2012) Direct leptin action on POMC neurons regulates glucose homeostasis and hepatic insulin sensitivity in mice. J Clin Investig 122(3):1000–1009. https://doi.org/10.1172/Jci59816
15. Dodd GT, Decherf S, Loh K, Simonds SE, Wiede F, Balland E, Merry TL, Munzberg H et al (2015) Leptin and insulin act on POMC neurons to promote the browning of white fat. Cell 160(1–2):88–104. https://doi.org/10.1016/j.cell.2014.12.022
16. Burke LK, Doslikova B, D'Agostino G, Greenwald-Yarnell M, Georgescu T, Chianese R, Martinez de Morentin PB, Ogunnowo-Bada E et al (2016) Sex difference in physical activity, energy expenditure and obesity driven by a subpopulation of hypothalamic POMC neurons. Molecular Metabolism 5(3):245–252. https://doi.org/10.1016/j.molmet.2016.01.005
17. Plum L, Rother E, Munzberg H, Wunderlich FT, Morgan DA, Hampel B, Shanabrough M, Janoschek R et al (2007) Enhanced leptin-stimulated Pi3k activation in the CNS promotes white adipose tissue transdifferentiation. Cell Metab 6(6):431–445. https://doi.org/10.1016/j.cmet.2007.10.012
18. Wang C, He Y, Xu P, Yang Y, Saito K, Xia Y, Yan X, Hinton A Jr et al (2018) TAp63 contributes to sexual dimorphism in POMC neuron functions and energy homeostasis. Nat Commun 9(1):1544. https://doi.org/10.1038/s41467-018-03796-7
19. Nohara K, Zhang Y, Waraich RS, Laque A, Tiano JP, Tong J, Munzberg H, Mauvais-Jarvis F (2011) Early-life exposure to testosterone programs the hypothalamic melanocortin system. Endocrinology 152(4):1661–1669. https://doi.org/10.1210/en.2010-1288
20. Bartel DP (2009) MicroRNAs: target recognition and regulatory functions. Cell 136(2):215–233. https://doi.org/10.1016/j.cell.2009.01.002
21. Pasquinelli AE (2012) MicroRNAs and their targets: recognition, regulation and an emerging reciprocal relationship. Nat Rev Genet 13(4):271–282. https://doi.org/10.1038/nrg3162
22. Lai EC (2002) Micro RNAs are complementary to 3′ UTR sequence motifs that mediate negative post-transcriptional regulation. Nat Genet 30(4):363–364. https://doi.org/10.1038/ng865
23. Rajman M, Schratt G (2017) MicroRNAs in neural development: from master regulators to fine-tuners. Development 144(13):2310–2322. https://doi.org/10.1242/dev.144337
24. Bian S, Xu TL, Sun T (2013) Tuning the cell fate of neurons and glia by microRNAs. Curr Opin Neurobiol 23(6):928–934. https://doi.org/10.1016/j.conb.2013.08.002
25. Gao FB (2008) Posttranscriptional control of neuronal development by microRNA networks. Trends Neurosci 31(1):20–26. https://doi.org/10.1016/j.tins.2007.10.004
26. Bak M, Silahtaroglu A, Moller M, Christensen M, Rath MF, Skryabin B, Tommerup N, Kauppinen S (2008) MicroRNA expression in the adult mouse central nervous system. Rna 14(3):432–444. https://doi.org/10.1261/rna.783108
27. Crepin D, Benomar Y, Riffault L, Amine H, Gertler A, Taouis M (2014) The over-expression of miR-200a in the hypothalamus of ob/ob mice is linked to leptin and insulin signaling impairment. Mol Cell Endocrinol 384(1–2):1–11. https://doi.org/10.1016/j.mce.2013.12.016
28. Derghal A, Djelloul M, Airault C, Pierre C, Dallaporta M, Troadec JD, Tillement V, Tardivel C, Bariohay B, Trouslard J, Mounien L (2015) Leptin is required for hypothalamic regulation of miRNAs targeting POMC 3′UTR. Front Cell Neurosci 9. doi:Artn 172 https://doi.org/10.3389/Fncel.2015.00172
29. Vinnikov IA, Hajdukiewicz K, Reymann J, Beneke J, Czajkowski R, Roth LC, Novak M, Roller A et al (2014) Hypothalamic miR-103 protects from hyperphagic obesity in mice. J Neurosci 34(32):10659–10674. https://doi.org/10.1523/JNEUROSCI.4251-13.2014
30. Schneeberger M, Altirriba J, Garcia A, Esteban Y, Castano C, Garcia-Lavandeira M, Alvarez CV, Gomis R et al (2012) Deletion of miRNA processing enzyme Dicer in POMC-expressing cells leads to pituitary dysfunction, neurodegeneration and development of obesity. Molecular Metabolism 2(2):74–85. https://doi.org/10.1016/j.molmet.2012.10.001
31. Bian S, Hong J, Li Q, Schebelle L, Pollock A, Knauss JL, Garg V, Sun T (2013) MicroRNA cluster miR-17-92 regulates neural stem

cell expansion and transition to intermediate progenitors in the developing mouse neocortex. Cell Rep 3(5):1398–1406. https://doi.org/10.1016/j.celrep.2013.03.037
32. Jin J, Kim SN, Liu X, Zhang H, Zhang C, Seo JS, Kim Y, Sun T (2016) miR-17-92 cluster regulates adult hippocampal neurogenesis, anxiety, and depression. Cell Rep 16(6):1653–1663. https://doi.org/10.1016/j.celrep.2016.06.101
33. Pollock A, Bian S, Zhang C, Chen Z, Sun T (2014) Growth of the developing cerebral cortex is controlled by microRNA-7 through the p53 pathway. Cell Rep 7(4):1184–1196. https://doi.org/10.1016/j.celrep.2014.04.003
34. Latreille M, Hausser J, Stutzer I, Zhang Q, Hastoy B, Gargani S, Kerr-Conte J, Pattou F et al (2014) MicroRNA-7a regulates pancreatic beta cell function. J Clin Invest 124(6):2722–2735. https://doi.org/10.1172/JCI73066
35. Madisen L, Zwingman TA, Sunkin SM, Oh SW, Zariwala HA, Gu H, Ng LL, Palmiter RD et al (2010) A robust and high-throughput Cre reporting and characterization system for the whole mouse brain. Nat Neurosci 13(1):133–140. https://doi.org/10.1038/nn.2467
36. Ma W, Fuentes G, Shi XH, Verma C, Radda GK, Han WP (2015) FoxO1 negatively regulates leptin-induced POMC transcription through its direct interaction with STAT3. Biochem J 466:291–298. https://doi.org/10.1042/Bj20141109
37. Liu XS, Chopp M, Wang XL, Zhang L, Hozeska-Solgot A, Tang T, Kassis H, Zhang RL et al (2013) MicroRNA-17-92 cluster mediates the proliferation and survival of neural progenitor cells after stroke. J Biol Chem 288(18):12478–12488. https://doi.org/10.1074/jbc.M112.449025
38. Reddy OL, Cates JM, Gellert LL, Crist HS, Yang ZH, Yamashita H, Taylor JA, Smith JA et al (2015) Loss of FOXA1 drives sexually dimorphic changes in urothelial differentiation and is an independent predictor of poor prognosis in bladder cancer. Am J Pathol 185(5):1385–1395. https://doi.org/10.1016/j.ajpath.2015.01.014
39. Li Z, Tuteja G, Schug J, Kaestner KH (2012) Foxa1 and Foxa2 are essential for sexual dimorphism in liver cancer. Cell 148(1–2):72–83. https://doi.org/10.1016/j.cell.2011.11.026
40. Hurtado A, Holmes KA, Ross-Innes CS, Schmidt D, Carroll JS (2011) FOXA1 is a key determinant of estrogen receptor function and endocrine response. Nat Genet 43(1):27–U42. https://doi.org/10.1038/ng.730
41. Sahu B, Laakso M, Ovaska K, Mirtti T, Lundin J, Rannikko A, Sankila A, Turunen JP et al (2011) Dual role of FoxA1 in androgen receptor binding to chromatin, androgen signalling and prostate cancer. EMBO J 30(19):3962–3976. https://doi.org/10.1038/emboj.2011.328
42. Yang YA, Yu J (2015) Current perspectives on FOXA1 regulation of androgen receptor signaling and prostate cancer. Genes & Diseases 2(2):144–151. https://doi.org/10.1016/j.gendis.2015.01.003
43. Salinero AE, Anderson BM, Zuloaga KL (2018) Sex differences in the metabolic effects of diet-induced obesity vary by age of onset. Int J Obes 42:1088–1091. https://doi.org/10.1038/s41366-018-0023-3
44. Medrikova D, Jilkova ZM, Bardova K, Janovska P, Rossmeisl M, Kopecky J (2012) Sex differences during the course of diet-induced obesity in mice: adipose tissue expandability and glycemic control. Int J Obes 36(2):262–272. https://doi.org/10.1038/ijo.2011.87
45. Seeger T, Fischer A, Muhly-Reinholz M, Zeiher AM, Dimmeler S (2014) Long-term inhibition of miR-21 leads to reduction of obesity in db/db mice. Obesity 22(11):2352–2360. https://doi.org/10.1002/oby.20852
46. Gaudet AD, Fonken LK, Gushchina LV, Aubrecht TG, Maurya SK, Periasamy M, Nelson RJ, Popovich PG (2016) miR-155 deletion in female mice prevents diet-induced obesity. Sci Rep 6:22862. https://doi.org/10.1038/srep22862
47. Schroeder M, Drori Y, Ben-Efraim YJ, Chen A (2018) Hypothalamic miR-219 regulates individual metabolic differences in response to diet-induced weight cycling. Molecular Metabolism 9:176–186. https://doi.org/10.1016/j.molmet.2018.01.015
48. Piwecka M, Glazar P, Hernandez-Miranda LR, Memczak S, Wolf SA, Rybak-Wolf A, Filipchyk A, Klironomos F et al (2017) Loss of a mammalian circular RNA locus causes miRNA deregulation and affects brain function. Science 357. https://doi.org/10.1126/science.aam8526
49. Garg N, Po A, Miele E, Campese AF, Begalli F, Silvano M, Infante P, Capalbo C et al (2013) microRNA-17-92 cluster is a direct Nanog target and controls neural stem cell through Trp53inp1. EMBO J 32(21):2819–2832. https://doi.org/10.1038/emboj.2013.214
50. Ebert MS, Sharp PA (2012) Roles for microRNAs in conferring robustness to biological processes. Cell 149(3):515–524. https://doi.org/10.1016/j.cell.2012.04.005
51. Leung AKL, Sharp PA (2010) MicroRNA functions in stress responses. Mol Cell 40(2):205–215. https://doi.org/10.1016/j.molcel.2010.09.027
52. Challis BG, Coll AP, Yeo GSH, Pinnock SB, Dickson SL, Thresher RR, Dixon J, Zahn D et al (2004) Mice lacking pro-opiomelanocortin are sensitive to high-fat feeding but respond normally to the acute anorectic effects of peptide-YY3-36. Proc Natl Acad Sci U S A 101(13):4695–4700. https://doi.org/10.1073/pnas.0306931